Spin persistence in an antiferromagnetic triangular Ising lattice under a magnetic field

Xiaoyan Yao, Shuai Dong, Kai Xia, Penglei Li, and Jun-Ming Liu*
Laboratory of Solid State Microstructures, Nanjing University, Nanjing 210093, China
and International Center for Materials Physics, Chinese Academy of Sciences, Shenyang 110016, China
(Received 20 March 2007; revised manuscript received 14 June 2007; published 27 July 2007)

In order to understand the steplike magnetization behaviors often observed in frustrated magnetic systems (e.g., $Ca_3Co_2O_6$ compound) at low temperature, we study the spin persistence effect of quenched two-dimensional triangular Ising lattice of antiferromagnetic order under magnetic field, using Monte Carlo simulations. The one-to-one correspondence between the spin blockings and magnetization steps is demonstrated, indicating the essential contribution of the spin frustration freezing to the steplike magnetization behavior. It is revealed that the steplike jumps of the magnetization occurring at several critical magnetic fields are activated by drastic suppression of the spin blocking at these fields. We investigate in detail the dynamic evolution of the spin persistence probability and corresponding spin configuration as a function of magnetic field, and it is indicated that the degree of spin activeness as determined by the energy change due to spin flips induces the stepwise behavior of the magnetization. This work presents a sound explanation to the steplike magnetization of $Ca_3Co_2O_6$ compound at low temperature.

DOI: 10.1103/PhysRevB.76.024435 PACS number(s): 75.50.Gg, 75.10.Hk, 75.30.Kz, 75.40.Mg

I. INTRODUCTION

The problem of order-parameter persistence (first passage) is an important aspect of nonequilibrium statistical dynamics in quite a number of condensed matter systems, such as coarsening phenomena[1] and fluctuating interfaces.[2] It has been receiving attention in recent years because of its essential significance in determining the evolution dynamics of phase transitions. In a general sense, this problem deals with the fraction of species in the order-parameter space which persists in its initial state (time $t=0$) up to some later time. Therefore, it allows us an unusual way to understand the time-dependent evolution and memory retaining effect of the initial state for a many-body interacting system.[3] For a spin lattice at zero temperature ($T=0$), the persistence problem focuses on the fraction of spins that persist their states for $t>0$ the same as the initial ones at $t=0$, i.e., the persistence probability $P(t)$ as a function of t following a deep quench from $T=\infty$ to $T=0$. In other words, the spin persistence can be quantified as the time dependent $P(t)$ that a spin maintains its initial state up to time t.[4] For the homogeneous ferromagnetic Ising lattice of dimension $d\leqslant 3$, $P(t)$ exhibits a power-law relaxation,[5–7] while for Ising lattice of $d>3$ (Ref. 7) or the q-state Potts lattice on two-dimensional (2D) square lattice ($q>4$),[8] the spin configuration will converge to a metastable state and a nonvanishing $P(t)$ appears as $t\rightarrow\infty$. The latter effect is regarded as the spin blocking and is also available in some spin models with disorder.[9–12] The persistence and blocking behaviors characterize the dynamical evolution of spin systems, benefiting to our understanding of the magnetic properties.

Recently, the geometrically frustrated spin systems have collected a lot of attention not only due to the complicated spin configurations of spin-frustrated systems but also for some fascinating effects associated with the spin frustration configurations, such as multistep magnetization and ferroelectricity as observed in quite a few of spin-frustrated transition-metal oxides.[13–16] The physics underlying these peculiar phenomena lies in the fact that the competing interactions in these spin-frustrated systems produce high degeneracy of states, in which the spin blocking effect may be expected. Along this line, the spin systems of antiferromagnetic (AFM) interaction and triangular lattice symmetry are of special interest and appropriate objects for investigating geometrical frustration of spins. For example, $Ca_3Co_2O_6$ compound is such a system which has been investigated both experimentally[16–18] and theoretically[19–21] due to the fundamental and technological significance. The spins align along the c axis and form one-dimensional spin chains due to the strong ferromagnetic interaction. These spin chains, which can be regarded as a rigid giant spin, construct triangular lattice in the ab plane with weak interchain AFM coupling, and then the resultant magnetic structure has typical 2D AFM triangular symmetry in the ab plane. One of the most fascinating features observed in $Ca_3Co_2O_6$ is the steplike magnetization (M) plotted against magnetic field (h) applied along the chains (the c axis) at low T. As T falls down into between 10 and 25 K, M presents a $M_0/3$ (where M_0 is that saturated magnetization) step upon h increasing from 0 to 3.6 T. Further increasing of h leads the jump of M up to M_0. Furthermore, as $T<10$ K, the $M_0/3$ plateau decomposes into three nonzero and equidistant substeps separated at $\sim$1.2 T, 2.4 T below 3.6 T, i.e., each step has a width of $\sim$1.2 T. For the $M_0/3$ plateau observed at $T\sim 10$ K, the ferrimagnetic scenario was accepted widely, but the origin of the multistep behavior at low T remains controversial.[16,18,22] In our earlier work,[21] the Monte Carlo simulation on a 2D triangular Ising model was performed, and the steplike M-h feature in $Ca_3Co_2O_6$ was reproduced in a quantitative sense. It was argued that the competition between the interchain AFM interaction and field h may be responsible for these peculiar behaviors.

Nevertheless, these works described above dealt mainly with the highly degenerated states and no dynamic aspect of the multistep magnetization has been addressed. We are basically interested in the spin flip dynamics during the evolu-

tion of the spin-frustrated lattice from a high-T state quenched toward the equilibrium state of $T=0$. In detail, it is helpful to understand how the multistep magnetization is evolved and what will happen between the neighboring two steps by investigating the spin persistence phenomenon during the spin lattice evolution. In this paper, the steplike behavior of M as a function of h for an AFM triangular lattice will be investigated from the point of view of the spin persistence. In fact, no much investigation on the persistence and blocking in spin-frustrated systems has been done, although Kim *et al.* once focused on this issue by simulating the persistence at zero field, showing an exponential decay of $P(t)$.[4] The more important issue should be associated with that under nonzero field, aiming at the steplike M. We report our simulation on the persistence behavior under different h. It is observed that the evolution of the spin configuration has different characters at different h. The one-to-one correspondence between the spin blocking and the magnetization plateau can be established. These results are believed to be informative for the understanding of the magnetic behavior in frustrated systems.

The remaining part of this paper is organized as follows. In Sec. II, we introduce the model and the method used to perform the simulations. In Sec. III, we present the results and discussion. Conclusion is presented in Sec. IV.

II. MODEL AND MONTE CARLO SIMULATION

We start from the simple 2D triangular lattice of the AFM interaction. As well established, the Hamiltonian of this lattice is given by

$$H = -\sum_{\langle m,n\rangle} JS_mS_n - h\mu_B g\sum_m S_m, \tag{1}$$

where $J<0$ is the AFM coupling factor between each nearest-neighboring spin pair, S_m is the effective Ising spin situated on every site of the triangular lattice with moment $\pm S$, $\langle m,n\rangle$ denotes the summation over all the nearest-neighboring pairs, and h is the magnetic field applied along the direction of up spins. For different materials, J and S should have different values, and the magnetic behavior of $Ca_3Co_2O_6$ at low T can be well described by this Hamiltonian with appropriate J and S, and for details, one may refer to Refs. 19–21. For convenience, we set $J=-1$ and $k_B=\mu_B=g=S=1$ throughout the paper.

The simulation starts from a 2D $L\times L$ ($L=2000$) triangular lattice with periodic boundary conditions, and the lattice dimension is large enough to gain satisfactory statistics. The evolution time (t) of the system is measured by Monte Carlo step (MCS). Each simulation run begins at $t=0$ with a random initial configuration (in which each spin is equally likely to be up or down, independent of the others). Then, let the system be quenched down to $T=0$ and evolve via single spin flip zero-temperature Glauber dynamics (hereafter, all the data are obtained by the Glauber algorithm except otherwise stated). In detail, we first calculate the energy change that would result from flipping a spin. Then, we update the lattice according to the following updating rule: the spin always flips if the energy change is negative, never flips if the energy change is positive, and flips at random if the energy change is zero, i.e., the flip probability is 1/2. Averages over more than ten different samplings were performed for each run undertaken.

The spin persistence probability defined over the whole lattice is

$$P(t) = n(t)/N, \tag{2}$$

where $n(t)$ is the number of spins which have never flipped until time t, which is monitored after practically each MCS. $N=L\times L$ is the total number of spins. In addition, we define the spin blocking probability (P_B) as

$$P_B = P(\infty). \tag{3}$$

In the simulation, P_B is the stable value of $P(t)$ extracted from $P(t)$ curves after $P(t)$ reaches a stable state. For the case of spin blocking, P_B has a nonzero value. Afterward, the magnetization M_p is evaluated by summing all the spins and normalized by N, i.e.,

$$M_p = \frac{1}{N}\sum_i S_i. \tag{4}$$

The simulation indicates that M_p will keep invariable when $P(t)$ reach a stable value. It must be noted here that M_p is calculated in the same way as P_B, which is slightly different from evaluated M in experiments and previous simulations.[17,18] It is used to characterize the magnetization with the spin persistence effect, which forms a bridge between the spin persistence and the observable magnetization M. At the same time, when M_p is calculated, the total energy of the system normalized by N is also evaluated as follows:

$$E_p = \frac{1}{N}\left(-\sum_{\langle m,n\rangle} JS_mS_n - h\mu_B g\sum_m S_m\right). \tag{5}$$

To explore the spin persistence further, we propose two dynamic parameters: the total number of the spin flips (TFT) and the distribution of the spin flip numbers (NDFT), which present more information on the dynamic behavior of the spin flipping and lattice evolution. Parameter TFT is the total number of spin flips accumulated from $t=0$ to t, depending on t, normalized by N. If the flip number of the spin at site i at time t is $n_i(t)$, then

$$\mathrm{TFT}(t) = \frac{1}{N}\sum_i^N n_i(t). \tag{6}$$

NDFT is also t dependent, showing different features at different t. For a given t, the number of spins which have flipped n_{FT} times is counted, namely,

$$\mathrm{NDFT}(n_{FT}) = \frac{1}{N}\sum_i^N \delta(n_i - n_{FT}). \tag{7}$$

Thus, the distribution function NDFT is obtained. It should be noted that the area under the curve of NDFT is always normalized to 1 by factor N.

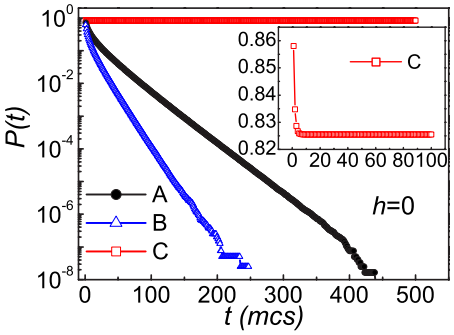

FIG. 1. (Color online) P as functions of t with different updating rules which are described in the text. The inset gives the enlargement of the curve of C.

III. RESULTS AND DISCUSSION

A. Effect of updating algorithm

Before presenting the details of the dynamics of spin persistence, we first briefly investigate the effect of the updating rules using different simulation algorithms. In Fig. 1 are plotted the simulated $P(t)$ as evaluated by three different algorithms under zero-field condition ($h=0$). Curve marked with A (solid dots) is from the Glauber algorithm. For reference purposes, the calculated $P(t)$ curves employing other two different updating rules are also presented in Fig. 1. For curve B (open triangular dots), the updating rule is that spins always flip unless the energy change is positive, while curve C (open square dots) results from the rule that no spin flip is possible unless the energy is reduced by such a flip.

It is seen that after the initial transient relaxation range ($t<80$ MCS) where $P(t)$ shows a relatively fast decrease, an exponential decay of $P(t)$ over the whole time range is displayed. Due to the finite lattice size, $P(t)$ becomes noisy at large t and then reaches zero, i.e., $P_B=0$. Curve B, as explained in Ref. 4, has faster decreasing rate than curve A. However, for curve C, as clearly shown in the inset of Fig. 1, except the sharp decline in the initial period, $P(t)$ preserves a large value ($P_B\sim0.8255$) which is maintained toward the long-time limit, i.e., $P_B>0$. This corresponds to the spin blocking effect, indicating that most of the spins are blocked after the initial short-time period. This result allows us to argue that the spin persistence in the present spin lattice has much thing to do with the algorithm employed for the updating. If the spin flipping without energy fluctuation is allowed even though with a very small but nonzero probability, $P_B\sim0$ is obtained, while the spin blocking appears otherwise. Nevertheless, it should be mentioned that the Glauber algorithm is a well-accepted rule which allows the random fluctuation of spins at $T=0$, consistent with realistic statistical systems. Therefore, all of the results presented below are obtained employing the Glauber algorithm.

B. Stepwise behavior of blocking probability

The spin persistence behavior with $P_B=0$ described above is very unstable against magnetic field, even though h takes extremely small value. In Fig. 2(a) are presented the $P(t)$ curves evaluated under several very small values of h. It is surprising to observe that the lattice is seriously blocked once a very weak field is applied. While $P_B\sim0$ is obtained at $h=0$, it jumps up to ~0.67 once h becomes nonzero and no matter how small h is (within the simulation uncertainties). It is also observed that P_B does not depend on h over a broad range and in the present lattice $P_B\sim0.67$ is retained until $h=2.0$ at which a jump of P_B occurs, to be shown later. Therefore, the spin blocking probability P_B as a function of h may reflect in an essential way the dynamic feature of the spin frustration in the present system. For the spins that eventually flip, the behavior of $p(t)=P(t)-P_B$ decays exponentially toward zero, namely,

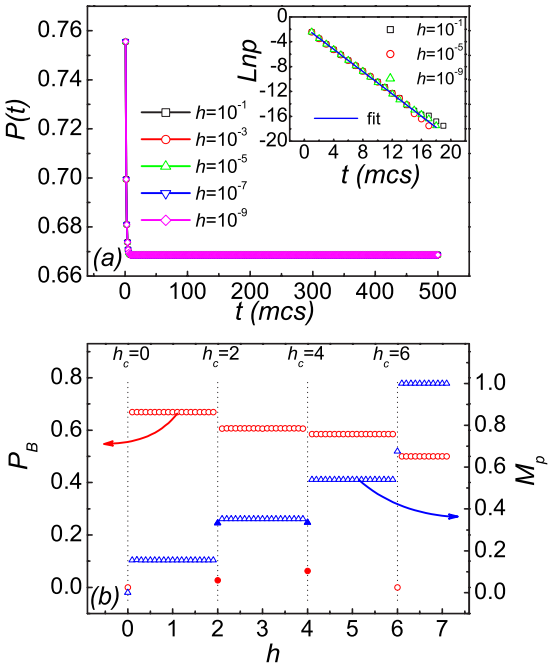

FIG. 2. (Color online) (a) P as functions of t at different h. The inset presents $\ln(p)$ versus t at different h and the solid line shows the fitting result of $p(t)$. (b) P_B and M_p as functions of h. Note that at $h_c=2$ and 4, the two red solid circles demonstrate the simulation results of P_B and the two blue solid triangles illustrate those of M_p after $t=100\,000$ MCS.

$$p(t) \propto \exp(-at). \tag{8}$$

As shown in the inset of Fig. 2(a), one can get $a=0.897\pm0.004$ from the fitting curve, according to Eq. (8).

In order to reveal the correspondence between the spin blocking behavior and the steplike magnetization, we simulate the two parameters, P_B and M_p, over a broad range of h ($h=0.0-7.0$), and the results are plotted in Fig. 2(b). In a general tendency, both P_B and M_p, as a function of h, respectively, show the stepwise behavior. As $h=0$, 2, 4, and 6, the four critical fields, jumping of P_B and M_p from one plateau to its neighboring one, respectively, are identified, demonstrating the perfect one-to-one correspondence between the two types of stepwise behaviors. Here, two interesting features regarding the stepwise behaviors should be pointed out. First, these plateaus have the same width of $\Delta h=2$, although

their heights differ from one another. The height of P_B plateau decreases with increasing h, reaching $P_B=1/2$ as $h>6.0$, noting that the minimal of P_B under $h\to\infty$ is 1/2. For M_p, the plateau height increases with h, reaching the maximal saturated $M_p=1.0$ as $h>6.0$. The multistep behavior of the magnetization has been well documented for $Ca_3Co_2O_6$ compound at $T=2$ K,[16,17] although the evaluated $M_p(h)$ here is calculated from a random initial state following a deep quench to $T=0$. Second, it is shown that at the four critical fields, $h_c=0$, 2, 4, and 6, both P_B and M_p have their values different from the plateaus at both sides, to be addressed later.

The equidistant distribution of these plateaus was observed experimentally for $Ca_3Co_2O_6$ compound and it may be due to the competition of the exchange interaction term and magnetic field term in the Hamiltonian.[20,21] When one spin S_i flips to $-S_i$, according to Eq. (1), the energy change (E_f) from the new state to the old one is

$$E_f = 2S_i\left(J\sum_n S_n + h\right). \tag{9}$$

Since only the flips with $E_f\leqslant 0$ are allowed, for $E_f=0$,

$$h_c = -J\left(\sum_n S_n\right). \tag{10}$$

The term in the parentheses on the right of the equation is the summation of the six nearest-neighbor spins, which could be $-6S$, $-4S$, $-2S$, $0S$, $2S$, $4S$, or $6S$. If $h\geqslant 0$ is assumed, $h=h_c=0$, 2, 4, and 6, with $J=-1$ and $S=1$. While for $h\neq h_c$, $M_p(h)$ and $P_B(h)$ must present the plateau feature, at $h=h_c$, M_p does not necessarily lie on any plateau and the spin persistence shows interesting anomalies by the P_B value far lower than those plateau values. In the following, the spin persistence behaviors under different h, especially the anomalies at h_c, will be discussed, respectively, in detail.

C. Persistence behavior under $h\neq h_c$

As $h\neq h_c$, M_p keeps on the plateaus and the lattice presents the spin blocking. Figure 3(a) shows the simulated $P(t)$ on the four plateaus shown in Fig. 2(b), respectively. The spin blocking behaviors for each case are similar but with different values of P_B which declines with increasing h. The reason is that the lattice evolves from the random initial state with half spins up and half down, so more down spins tend to flip up under higher h. Correspondingly, parameter TFT is also calculated, as shown in Fig. 3(b). At the initial time period, it shows a sharp rise and then keeps on a constant value, indicating that a constant fraction of spins never flips and the other spins flip with finite times. Consequently, the spins remain "dead" under h except at $h_c=0$, 2, 4, and 6. The reason for the spin blocking is that after the initial time period the event with $E_f<0$ will no more appear if $h\neq h_c$. According to the Glauber dynamics, only the spin flipping of $E_f\leqslant 0$ is permitted, so as $h\neq h_c$, only those flips with reduced energy can occur. Since every spin flip event lowers the energy, the total lattice energy will monotonically decrease in time and eventually no more energy reduction can be possible after a finite time period,[9] thus reaching the blocking, i.e., the metastable states originating from the high degeneracy of states due to the geometrical frustration. Between any two neighboring h_c (i.e., $0\to 2$, $2\to 4$, $4\to 6$, and above 6), variation of h can no longer affect the sign of E_f, leading to the plateau formation of $P_B(h)$ and $M_p(h)$.

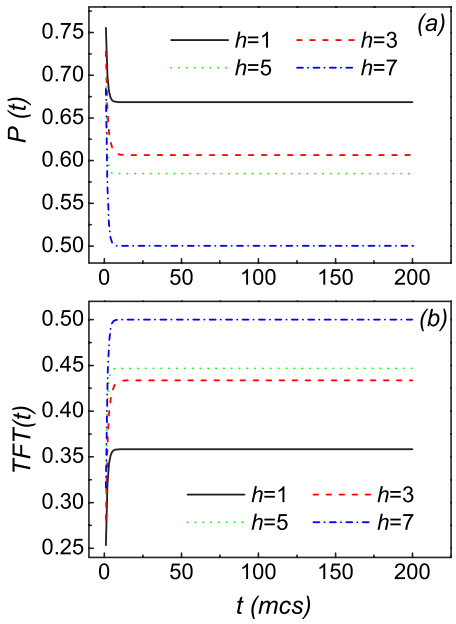

FIG. 3. (Color online) (a) P and (b) TFT as functions of t at different h.

D. Persistence behavior under $h=h_c$

Now, we study the abnormal persistence behaviors at the four critical fields, $h_c=0$, 2, 4, and 6. It is observed that at $h_c=0$ and 6, the lattice has similar persistence behaviors, as demonstrated in Fig. 4(a), differing from those at $h_c=2$ and 4. After a quick decline, $P(t)$ at both $h_c=0$ and 6 exhibits an exponential relaxation

$$P(t)\propto \exp(-at). \tag{11}$$

Equation (11) is used to fit our data and a good fitting is achieved with different factor a ($a=0.035\,62\pm0.000\,02$ for $h_c=0$ and $a=0.067\,37\pm0.000\,01$ for $h_c=6$), as shown in Fig. 4(a) where the dot lines are the fitting curves. The simulated TFT(t) is presented in the inset of Fig. 4(a), presenting a linear increase with t. The inset of Fig. 4(b) presents the evaluated NDFT at $t=1000$ MCS, showing a smooth and single-peak pattern for both $h_c=0$ and 6. The peak at $h_c=6$ is higher and sharper than that at $h_c=0$, shifting to the right side, which corresponds to the faster decay of $P(t)$ at $h_c=6$ than that at $h_c=0$. The evaluated NDFT curves at different t with $h_c=0$ are plotted in Fig. 4(b). With increasing t, the peak moves rightward and gradually becomes lower and broader. From these results, one can conclude that no blocking appears and every spin remains active at $h_c=0$ and 6. Therefore, at $h_c=0$ and 6, the spin flipping is very active and the lattice evolves without an end.

The spin persistence behaviors at $h_c=2$ and 4 are different from those at $h_c=0$ and 6. As shown in Fig. 5(a), $P(t)$ fol-

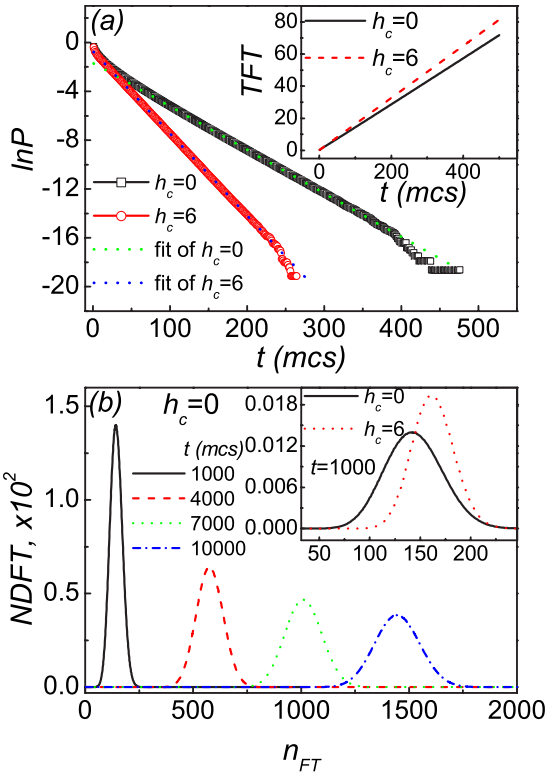

FIG. 4. (Color online) (a) ln P against t under h_c=0 and 6. The dotted line is the fit to the data after discarding the initial short-time behavior. The inset gives TFT(t) curve correspondingly. (b) NDFT at different t with h_c=0. NDFT curves for h_c=0 and 6 at t =1000 MCS are illustrated in the inset.

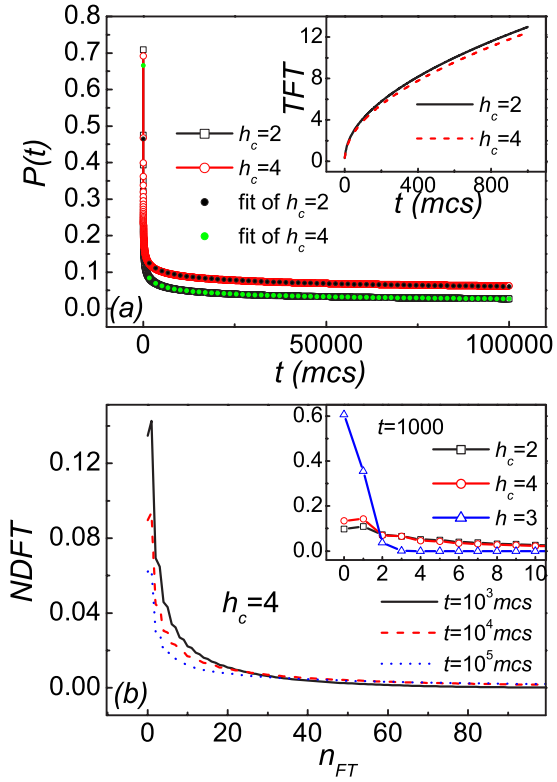

FIG. 5. (Color online) (a) ln P versus t at h_c=2 and 4. The dotted lines show the fitting results of $P(t)$ throughout whole t range. TFT(t) curve is shown as the inset. (b) NDFT at different t with h_c=4. NDFT curves for h_c=2, 4, and h=3 at t=1000 MCS are illustrated in the inset.

lows a power law, as well demonstrated earlier:[5–7]

$$P(t) \propto t^{-\theta}, \tag{12}$$

where θ is the persistence exponent. The fitting curves show θ=0.277 85±0.000 02 for h_c=2 and θ=0.176 40±0.000 08 for h_c=4. In the inset of Fig. 5(a), TFT(t) shows a nonlinear raising, namely, the spins flip more and more slowly. In the inset of Fig. 5(b) are the evaluated NDFT curves at h_c=2 and 4, which do not show any peak pattern as shown for h_c=0 and 6. These curves are also different from the blocking case, e.g., that at h=3 presented in the inset of Fig. 5(b) as a reference. In addition, no significant shift of the NDFT curve is observed with increasing t. Since Eq. (12) shows a trend to zero as $t \to \infty$, no spin blocking is possible. The very slow decaying of $P(t)$ leads to such a fact that the lattice evolves so slowly and the saturation of $P(t)$ cannot be reached even after t=100 000 MCS. Thus, in Fig. 2(b), we use the solid dots to represent the evaluated $P_B(h=2)$ and $P_B(h=4)$ (red solid circles) $M_p(h=2)$ and $M_p(h=4)$ (blue solid triangles) after $t=10^5$ MCS.

These abnormal spin persistence features described above result from the interesting physics associated with the Glauber dynamics. At $h=h_c$, the spin flip with E_f=0 exists. Given a time t, some spins can flip without any energy cost. Their flips may lead to the same events (E_f=0) of those neighboring spins at time $t+\Delta t$. This feature is typical for the spin-frustrated systems and also the reason why $P(t)$ can approach to zero and no spin blocking is possible. Besides, as shown in Figs. 6(a) and 6(b), the snapshot of spin configurations at h_c=2 and 4 at $t=10^5$ MCS approach the ferrimagnetic state, namely, one of the three spins takes spin down, while the other two take spin up, leading $M_p \sim M_0/3$, as marked by the blue solid triangles in Fig. 2(b). This anomaly can also be understood by E_p as a function of h, as shown in Fig. 6(c). While $E_p(h)$ behaves as straight lines between two neighboring critical fields, its values at h_c=2 and 4 are not on the straight lines. For reference purposes, the energy of the ferrimagnetic state under different h, i.e., $E_{FI}(h)$, is calculated according to Eq. (5). Owing to the regular spin configuration of the ferrimagnetic state, namely, one-third of the spins take spin down and are surrounded by six up spins, and the two-thirds of them are spin up with half neighbors spin up and half spin down, E_{FI} can be written as

$$E_{FI} = \frac{1}{N}\left\{\frac{1}{3}\left[-\frac{1}{2}(-1)6(-1)-(-1)h\right] + \frac{2}{3}\left[-\frac{1}{2}(-1)0\ 1-1h\right]\right\} = \frac{1}{N}\left(-1-\frac{h}{3}\right). \tag{13}$$

Equation (13) is plotted in Fig. 6(c) as the solid line. We can find that the evaluated E_p from the simulation at h_c fall exactly on this line. In the h range from 0 to 6, E_{FI} is lower

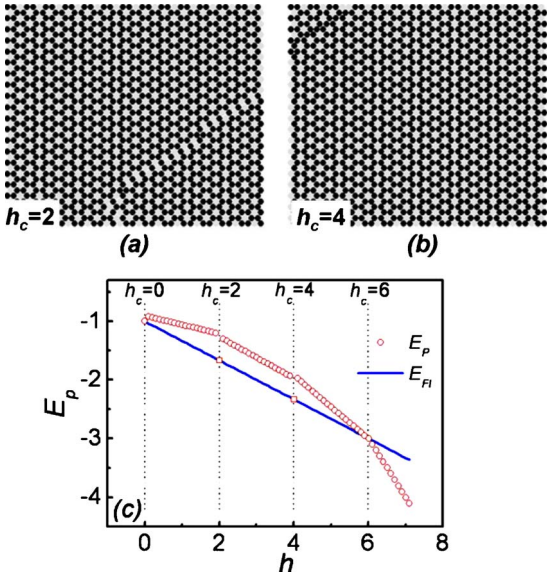

FIG. 6. (Color online) 40×40 spin snapshot of the triangular lattice for (a) $h_c=2$ and (b) $h_c=4$. (c) E_P as a function of h obtained from our simulations is denoted by red empty circles. Note that at $h_c=2$ and 4, the two red empty squares demonstrate the simulation results of E_P after $t=100\,000$ MCS. For reference purposes, E_{FI} against h calculated from Eq. (13) is plotted by the blue solid line.

than E_p. However, over the whole h range except $h=h_c$, the lattice evolves following E_p instead of E_{FI}. The reason is that the spin configurations are frozen into the metastable states. However, if $h=h_c$, the spins are not frozen and E_p must fall onto the E_{FI}-h line. The points at $h_c=0$ and 6 are the intersections of $E_p(h)$ and $E_{FI}(h)$, but for $h_c=2$ and 4, the lattice needs more time to reach E_{FI} because of the nonzero gap between $E_P(h)$ and $E_{FI}(h)$. This explains why the lattice evolution at $h_c=2$ and 4 is more slowly than that at $h_c=0$ and 6. It may be expected that in the long-time limit, P_B at $h_c=2$ and 4 will eventually approach zero and M_p will reach 1/3, corresponding to the perfect ferrimagnetic spin configuration.

E. Discussion about $Ca_3Co_2O_6$

The investigation of persistence phenomenon mentioned above reflects the underlying physics of the steplike M observed in experiments. In $Ca_3Co_2O_6$, equidistant steps separated at four critical fields $h'_c=0$, 1.2, 2.4, and 3.6 T (corresponds to $h_c=0$, 2, 4, and 6 in the present simulation) are observed at very low T such as 2 K. According to the above analyses, when $h\neq h'_c$, the flipping of spin is not active, the spin configurations are frozen into metastable states, and M as a function of h shows the steps. When $h=h'_c$, the spins are very active, so $M(h)$ jumps from one step to another. Since this multistep behavior is due to that the system is frozen into the metastable states, the measured M-h dependence upon the field increasing and then field decreasing cycle is hysteretic under the quasistatic magnetic fields.[17] As T increases, the spins have more opportunities to flip due to the thermal activation, so the frozen states melt gradually and more spins can reach the ferrimagnetic state. At about 10 K, in the whole h range from 0 to 3.6 T, the system shows the ferrimagnetic state and M presents a $M_0/3$ large plateau before the jump to M_0 at 3.6 T. Besides, no hysteresis can be observed above about 10 K. As T is raised further, the thermal fluctuation washes out all the steps gradually. In other words, the T-dependent magnetization behaviors against h at low temperature observed in $Ca_3Co_2O_6$ can be well understood based on the investigation of nonequilibrium dynamics in this work, which will also be very helpful to comprehend the complex magnetic properties observed in other frustrated materials.

IV. CONCLUSION

In summary, the spin persistence effect of a 2D AFM Ising model in a triangular lattice under the magnetic field is extensively investigated using Monte Carlo simulations. In the h range from 0 to 7, different persistence behaviors are investigated. The one-to-one correspondence between the spin blockings and magnetization steps is demonstrated with four critical magnetic fields $h_c=0,2,4,6$. It is indicated that E_f is an important factor to decide the persistence behavior and then the magnetic properties. When the spin flipping with $E_f=0$ is impossible, the spins are not active and then the blocking appears. For $M_P(h)$ curve, plateaus emerge. When the spin flipping of $E_f=0$ is possible for some certain h (h_c), some spins can flip with zero energy consumption. Therefore, the spins are very active and there is no blocking at these h_c. For $M_P(h)$ curve, these h_c are the critical points of steps.

ACKNOWLEDGMENTS

The authors thank the National Natural Science Foundation of China (Grants No. 10674061 and No. 50332020) and the National Key Projects for Basic Research of China (Grants No. 2002CB613303 and No. 2006CB921802).

*Corresponding author. liujm@nju.edu.cn

[1] A. J. Bray, Adv. Phys. **43**, 357 (1994).
[2] J. Krug, H. Kallabis, S. N. Majumdar, S. J. Cornell, A. J. Bray, and C. Sire, Phys. Rev. E **56**, 2702 (1997).
[3] S. N. Majumdar and A. J. Bray, Phys. Rev. Lett. **91**, 030602 (2003).
[4] E. Kim, B. Kim, and S. J. Lee, Phys. Rev. E **68**, 066127 (2003).
[5] B. Derrida, A. J. Bray, and C. Godreche, J. Phys. A **27**, L357 (1994).
[6] B. Derrida, V. Hakim, and V. Pasquier, Phys. Rev. Lett. **75**, 751 (1995).
[7] D. Stauffer, J. Phys. A **27**, 5029 (1994).

[8] B. Derrida, P. M. C. d. Oliveira, and D. Stauffer, Physica A **224**, 604 (1996).
[9] C. M. Newman and D. L. Stein, Phys. Rev. Lett. **82**, 3944 (1999).
[10] S. Jain, Phys. Rev. E **60**, R2445 (1999).
[11] S. Jain, Phys. Rev. E **59**, R2493 (1999).
[12] S. Jain and H. Flynn, Phys. Rev. E **73**, 025701(R) (2006).
[13] K. Taniguchi, N. Abe, T. Takenobu, Y. Iwasa, and T. Arima, Phys. Rev. Lett. **97**, 097203 (2006).
[14] M. A. Subramanian, T. He, J. Chen, N. S. Rogado, T. G. Calvarese, and A. W. Sleight, Adv. Mater. (Weinheim, Ger.) **18**, 1737 (2006).
[15] N. Ikeda *et al.*, Nature (London) **436**, 1136 (2005).
[16] V. Hardy, M. R. Lees, O. A. Petrenko, D. McK. Paul, D. Flahaut, S. Hébert, and A. Maignan, Phys. Rev. B **70**, 064424 (2004).
[17] H. Kageyama, K. Yoshimura, K. Kosuge, M. Azuma, M. Takano, H. Mitamura, and T. Goto, J. Phys. Soc. Jpn. **66**, 3996 (1997).
[18] A. Maignan, C. Michel, A. C. Masset, C. Martin, and B. Raveau, Eur. Phys. J. B **15**, 657 (2000).
[19] Y. B. Kudasov, Phys. Rev. Lett. **96**, 027212 (2006).
[20] X. Y. Yao, S. Dong, and J.-M. Liu, Phys. Rev. B **73**, 212415 (2006).
[21] X. Y. Yao, S. Dong, H. Yu, and J.-M. Liu, Phys. Rev. B **74**, 134421 (2006).
[22] A. Maignan, V. Hardy, S. Hebert, M. Drillon, M. R. Lees, O. Petrenko, D. M. K. Paul, and D. Khomskii, J. Mater. Chem. **14**, 1231 (2004).